Trends Neurosci. 12, 462-467.
Rashin, A. A, & Honig, B. (1985) *J. Phys. Chem. 89*, 5588-5593.
Sandberg, W. S., & Terwilliger, T. C. (1991) *Trends Biotechnol. 9*, 59-63.
Sanger, F., Miklen, S., & Coulson, A. R. (1977) *Proc. Natl. Acad. Sci. U.S.A. 74*, 5463-5467.
Satyshur, K. A., Sambhorao, T. R., Pyzalska, D., Drendall W., Greaser, M., & Sundaralingam, M. (1988) *J. Biol. Chem. 263*, 1628-1647.
Sekharadu, Y. C., & Sundaralingam, M. (1988) *Protein Eng. 2*, 139-146.
Shannon, R. D. (1976) *Acta Crystallogr. A32*, 751-767.
Snyder, E. E., Buosci, B. W., & Falke, J. J. (1990) *Biochemistry 29*, 3937-3943.
Strynadka, N. C., & James, M. N. G. (1989) *Annu. Rev. Biochem. 58*, 951-998.
Sussman, F., & Weinstein, H. (1989) *Proc. Natl. Acad. Sci. U.S.A. 86*, 7880-7884.
Tabor, S., & Richardson, C. C. (1987) *Proc. Natl. Acad. Sci. U.S.A. 84*, 4767-4771.
Tsien, R. W., Hess, P., McCleskey, E. W., & Rosenberg, R. L. (1987) *Annu. Rev. Biophys. Biophys. Chem. 16*, 265-290.
Vieira, J., & Messing, J. (1987) *Methods Enzymol. 153*, 5463-5467.
Vyas, N. K., Vyas, M. N., & Quiocho F. A. (1987) *Nature 327*, 635-638.
Vyas, M. N., Jacobson, B. L., & Quiocho, F. A. (1989) *J. Biol. Chem. 264*, 20817-20821.

Determination of the Three-Dimensional Solution Structure of Barnase Using Nuclear Magnetic Resonance Spectroscopy

Mark Bycroft,*,‡ Svend Ludvigsen,§ Alan R. Fersht,‡ and Flemming M. Poulsen*,§

Cambridge Centre for Protein Engineering, University Chemical Laboratory, Lensfield Road, Cambridge, CB2 1EW U.K., and Department of Chemistry, Carlsberg Laboratory, Gamle Carlsberg Vej 10, DK 2500 Valby, Copenhagen, Denmark

Received March 22, 1991; Revised Manuscript Received June 14, 1991

ABSTRACT: The solution conformation of the ribonuclease barnase has been determined by using ^{1}H nuclear magnetic resonance (NMR) spectroscopy. The 20 structures were calculated by using 853 interproton distance restraints obtained from analyses of two-dimensional nuclear Overhauser spectra, 72 ϕ and 53 χ_1 torsion angle restraints, and 17 hydrogen-bond distance restraints. The calculated structures contain two α-helices (residues 6-18 and 26-34) and a five-stranded antiparallel β-sheet (residues 50-55, 70-75, 85-91, 94-101, and 105-108). The core of the protein is formed by the packing of one of the α-helices (residues 6-18) onto the β-sheet. The average RMS deviation between the calculated structures and the mean structure is 1.11 Å for the backbone atoms and 1.75 Å for all atoms. The protein is least well-defined in the N-terminal region and in three large loops. When these regions are excluded, the average RMS deviation between the calculated structures and the mean structure for residues 5-34, 50-56, 71-76, 85-109 is 0.62 Å for the backbone atoms and 1.0 Å for all atoms. The NMR-derived structure has been compared with the crystal structure of barnase [Mauguen et al. (1982) *Nature* (*London*) *297*, 162-164].

Bacillus amyloliquefaciens produces a small extracellular ribonuclease (M_r 12382) known as barnase (Hartley, 1989). Barnase is not homologous with pancreatic ribonuclease but does have some sequence and structural homology to a number of other microbial purine-specific ribonucleases (Hill et al., 1983). The gene coding for barnase has been cloned and the protein has been expressed in *Escherichia coli* (Padden & Hartley, 1987). Barnase has proved a good model system for studying the factors affecting protein stability and the pathway of protein folding (Kellis et al., 1988, 1989; Sali et al., 1988; Serrano & Fersht, 1989; Matouschek et al., 1989, 1990; Bycroft et al., 1990a). To complement these studies, we have embarked on an investigation of barnase using nuclear magnetic resonance spectroscopy.

The development of 2D NMR methods (Ernst et al., 1987) has enabled essentially complete assignments to be made of the ^{1}H NMR spectra of small proteins (Wüthrich, 1986). Once assignments are available, it is possible to analyze two-dimensional NOE spectra to obtain a set of interproton distances that can, in conjunction with torsion angle data obtained from J coupling constants, be used to calculate a solution conformation of the protein (Wüthrich, 1989; Clore & Gronenborn, 1989).

We have recently reported assignments of the majority of the ^{1}H NMR spectrum of barnase (Bycroft et al., 1990b). In this paper, we describe the calculation of the solution conformation of the protein on the basis of NMR data.

Experimental Procedures

Recombinant barnase was purified from a culture of *E. coli* containing the plasmid pMT410 (Paddon & Hartley, 1987) as described previously (Mossakowska et al., 1989). Samples contained 5 mM protein, pH 4.5, in either 90% H_2O/10% D_2O or 99.96% D_2O. Spectra were recorded at 37 °C on a Bruker AM 500 spectrometer. Phase-sensitive spectra were obtained by using both the time-proportional phase incrementation method (Marion & Wüthrich, 1983) and the hypercomplex method (States et al., 1982). NOESY (Jeener et al., 1979) and DQF-COSY (Piantini et al., 1982; Rance et al., 1983) spectra were recorded with 512 t_1 increments each with 2048 complex data points. Mixing times of 50, 100, and 150 ms were used in the NOESY experiments. The experimental data were zero filled to give a 8K × 2K data matrix. The data were

‡ Cambridge Centre for Protein Engineering.
§ Carlsberg Laboratory.

0006-2960/91/0430-8697$02.50/0

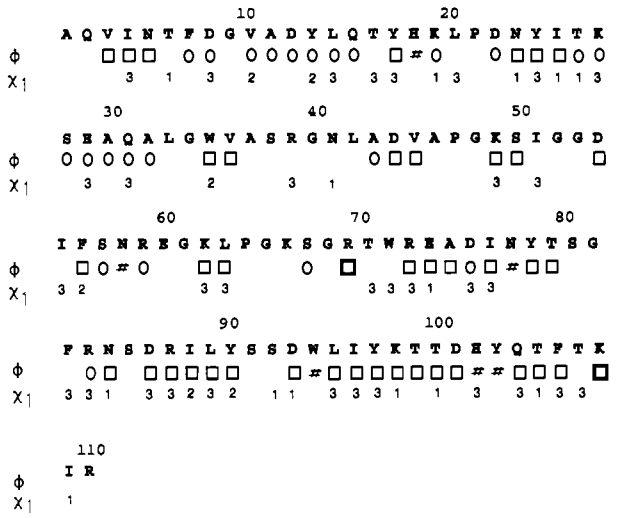

FIGURE 1: Diagrammatic representation of the angle constraints used in calculating the solution conformation of barnase. Symbols: (○) ${}^3J_{H^NH^\alpha} < 5.5$ Hz with ϕ constrained to the range −30° to −70°. (□) ${}^3J_{H^NH^\alpha} > 8.0$ Hz with ϕ constrained to the range −80° to −160°. (#) ϕ constrained to the range 10° to 110°. 1, 2, and 3 represent χ_1 dihedral angle restraints of (0, 120), (120, −120), and (0, −120), respectively.

processed with sine bells shifted by $\pi/12$ in f_2 and $\pi/9$ in f_1. The quality of the NOESY data has been illustrated previously. (Bycroft et al., 1990b).

Distance Restraints. Assignments for the majority of the protons in the ^{1}H NMR spectra of barnase have been reported previously (Bycroft et al., 1990b). In the course of this study, a few additional assignments for side-chain protons were made. A set of 853 interproton distance restraints were obtained from the analysis of NOESY spectra. The restraints are comprised of 294 intraresidue distances, 271 short-range $[(i - j) \leq 4]$ interresidue distances and 288 long-range $[(i - j) \geq 5]$ interresidue distances. The restraints were classified into distance ranges 1.8–2.7, 1.8–3.3, and 1.8–5.0 Å, corresponding to strong, medium, and weak NOEs, by counting the number of contour levels in the cross peaks. For NOEs involving methyl residues, an additional 0.5 Å was added to the upper limit (Wagner et al., 1987).

Angle Restraints. ${}^3J_{H^NH^\alpha}$ coupling constants were measured from H^N–H^α peaks by a method that relies on coupling information present in both DQF-COSY and NOESY spectra (Ludvigsen et al., 1991). Backbone ϕ angle constraints were obtained for 72 residues by using the Karplus (1963) relationship (Pardi et al., 1984). For ${}^3J_{H^NH^\alpha} < 5.5$ Hz, the ϕ angle constraint was $-70 < \phi < -30$, and for ${}^3J_{H^NH^\alpha} > 10$ Hz the ϕ angle constraint was $-150 < \phi < -90$. For six residues, a coupling constant greater than 6.0 Hz was observed together with a strong H^N–H^α intraresidue NOE. These interactions are consistent with a positive ϕ angle (Wüthrich, 1986), and for these residues the ϕ angle was constrained to the range 30–90° (Kline et al., 1988; Ludvigsen et al., 1991).

Stereospecific assignments for side-chain protons and χ_1 dihedral angle restraints were obtained by using intraresidue NOE effects and J coupling information as described by Arseniev et al. (1988) and Zuiderweg et al. (1985). The angle restraints used in the calculations are summarized in Figure 1. NOE information used in obtaining χ_1 constraints was not included in the rest of the structure calculation.

Hydrogen-Bonding Restraints. In the structure calculations, 34 distance restraints were included corresponding to the 17 hydrogen bonds that were identified previously, on the basis of NOE and amide-exchange data (Bycroft et al., 1990b).

FIGURE 2: Superposition of the backbone atoms of the 20 solution structures of barnase.

Protocol for Structure Calculations. Structures were calculated by using a two-stage distance geometry/simulated annealing procedure (Nilges et al., 1988). Initially, the metric matrix distance geometry program DISGEO (Havel, 1986) was used to generate a structure that contained only a subset of the atoms in the molecule. The rest of the atoms were then fitted, one residue at a time, to the substructure. This structure was then used as a starting point for dynamic simulated annealing calculations. Simulated annealing was carried out with the program XPLOR (Brünger, 1988), which is based on the molecular dynamics program CHARMM (Brooks et al., 1983). The annealing protocol used was essentially that described by Nilges et al. (1988). After minimization of the fitted structures without the NOE and torsion angle restraints, two periods of dynamics were carried out at 1000 K (3.75 ps) and 300 K (1.5 ps). In these calculations, a simplified energy function was used that contains only terms for bond lengths, bond angles, and improper torsions, a simple repulsion term, and square-well potentials to represent the NOE and torsion angle restraints (Nilges et al., 1988). During the 1000 K dynamics, the values of the force constants of the NOE, repulsion, and torsion angle terms were gradually increased from 1 to 50 kcal·mol^{-1}·Å^{-2}, 0.01 to 4 kcal·mol^{-1}·Å^{-4} and 5 to 200 kcal·mol·rad^{-2}, respectively. The resulting structures were finally subjected to a thousand cycles of restrained minimization with the full CHARMM energy function. The DISGEO calculations were carried out on a VAX 11/750 computer and XPLOR calculations on a Stardent 1500 computer. Structures were visualised on an Evans and Sutherland PS 390 using the program FRODO (Jones, 1978) or on a Stardent 1500 computer.

Results and Discussion

A total of 20 structures were calculated by using the restraints described above. The superposition of the backbone atoms of the structures are shown in Figure 2. The structures are well defined except for the first three amino acids for which there are only sequential NOE contacts. The average RMS deviation from the mean structure is 1.11 Å for the backbone atoms and 1.75 Å for all atoms. The average atomic RMS deviation between the calculated structures and the mean structure vs residue number is shown in Figure 3.

The calculated structures are in good agreement with the experimental data (Table I). None of the structures have violations of the NOE constraints greater than 0.4 Å, and the

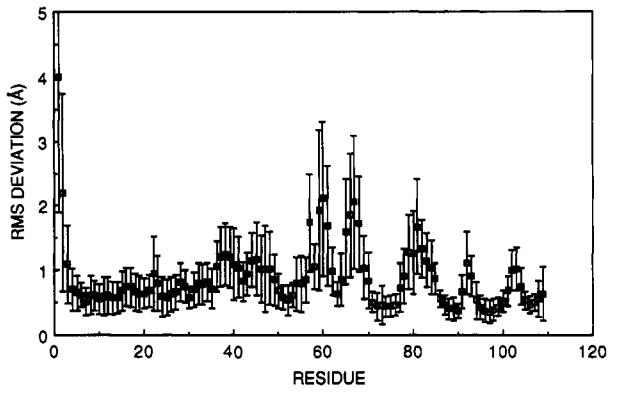

FIGURE 3: Average atomic RMS deviation from the mean structure for the 20 structures versus residue number.

Table I: Structural Statistics

	mean	range
RMS Deviations from NOE Restraints (Å)		
short range (271)	0.039	0.003
long range (288)	0.027	0.003
RMS Deviations from the Idealized Geometry Used within XPLOR		
bonds (Å)	0.0132	0.0004
angles (deg)	3.42	0.11
improper (deg)	11.00	0.28
XPLOR Potential Energies (kcal·mol^{-1})[a]		
E(VDW)	-468.82	10.18
E(NOE)	32.89	4.63
E(CDHI)	3.59	1.08

[a] The force constants of the NOE, repulsion, and torsion angle terms wre 50 kcal·mol^{-1}·Å^{-2}, 4 kcal·mol^{-1}·Å^{-4}, and 200 kcal·mol·rad^{-2}, respectively.

RMS deviation from the NOE restraints is 0.03 Å. The structures have good nonbonded contacts as evidenced by a negative value of the average van der Waals energy term (-472 kcal·mol^{-1}) and have small deviations from ideal geometry (Table I).

Description of the Structures. Elements of secondary structure were identified from characteristic hydrogen-bonding patterns (where the criteria for a hydrogen bond is that the CO–NH distance is less than 3.3 Å and the N–H–O angle is greater than 130°) and from average backbone torsion angles. Turns in the protein were identified when i, i+3 hydrogen bonds are present in all of the structures and were classified into types based on characteristic coupling constants and NOE patterns (Wüthrich, 1986).

The calculated structures contain two α-helices in the N-terminal third of the protein, on the basis of the presence of CO–NH$_{i+3}$ and CO–NH$_{i+4}$ hydrogen bonds. The first helix (α-I) extends from residue 6 to 18, on the basis of the hydrogen bonds present. The backbone ϕ angles of residues Tyr-17 and His-18, however, deviate significantly from those normally found in helices, as Tyr-17 has a large ϕ angle (-112°) and His-18 has a positive ϕ angle (46°). The second helix (α-II) extends from Thr-26 to Gly-34 and is more regular. All of the residues have backbone angles close to the typical helical values. The two helices are linked by a loop that contains a type I turn formed by residues 21–24.

The protein contains a five-stranded antiparallel β-sheet in the C-terminal portion consisting of residues 50–55 (β-I), 70–75 (β-II), 85–91 (β-III), 94–101 (β-IV), and 105–108 (β-V) (Figure 4). The hydrogen bonding in the β-sheet is regular except in the strand formed by residues 50–55, which contains a β-bulge at residues 53 and 54 (Richardson, 1981). The secondary structure is essentially the same as that previously identified by NMR (Bycroft et al., 1990b).

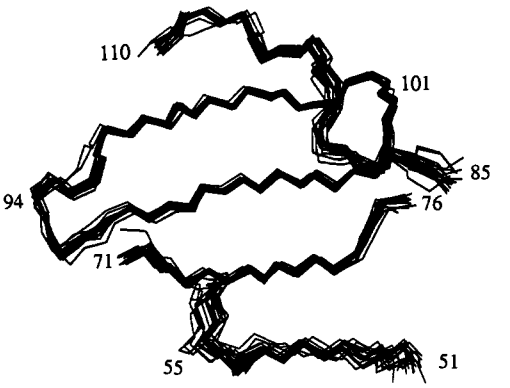

FIGURE 4: Superposition of the backbone atoms of the 20 solution structures of barnase showing the five-stranded antiparallel β-sheet.

FIGURE 5: Superposition of the side-chain atoms of residues Phe-7, Val-10, Leu-14, Ile-88, Tyr-90, and Ile-96 and the backbone atoms of the five-stranded β-sheet and the α-helix formed by residues 6–18 in the solution structure of barnase. Backbone atoms are shaded, and the side chains are in bold.

Strands III and IV of the β-sheet are linked by a type I turn and strands β-IV and β-V of the β-sheet are linked by a type III′ turn (Venkatachalam, 1968). The other strands of the β-sheet are linked by loops containing 15 residues (between β-I and β-II) and 10 residues (between strands β-II and β-III).

The core of the protein is formed by the packing of helix I onto the antiparallel β-sheet. This occurs in a manner typical of many α + β proteins and involves the interdigitation of hydrophobic residues in the helix and β-sheet (Chothia, 1984). Many NOE contacts are observed between protons in hydrophobic side chains in the α/β interface, and this region is one of the best defined in the solution structures (Figure 5). For residues 5–18, 50–56, 71–76, 85–100, and 105–109, the average RMS deviation from the mean structure is 0.54 Å for the backbone atoms and 0.94 Å for all atoms. The second helix packs against the edge of the β-sheet.

Three loops protrude from the central core of the protein. The loop between sheets β-I and β-II packs onto the β-sheet on the side opposite from helix α-I. The packing of the loop onto the β-sheet mainly involves the interaction of the side chain of Leu-63 with a hydrophobic pocket consisting of

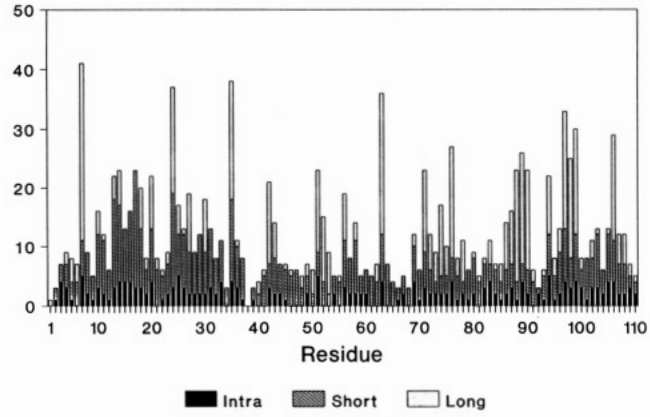

FIGURE 6: Schematic diagram showing the distribution of the NOE restraints used in the structure calculations.

residues Phe-56, Trp-71, Leu-89, Tyr-97, Tyr-103, and Phe-106. Many NOE contacts are seen from protons in the side chain of Leu-63 to protons in these residues. This loop is conserved in a number of related ribonucleases and is believed to be involved in the binding of substrate (Sevcik et al., 1990).

Residues 102, 73, and 87 have been implicated in the catalytic mechanism of barnase on the basis of sequence comparison studies of related ribonucleases (Hill et al., 1983) and by site-directed mutagenesis (Mossakowska et al., 1989). In the solution structures, these amino acids are located in a shallow groove in the protein. Residues 73 and 87 are in the β-sheet, and His-102 is in the turn containing residues 101–104.

The loops linking helix α-II and strand β-I and strains β-III and β-IV are on the opposite side of the core from the substrate-binding loop. The loop formed by amino acids 76–84 is in an extended conformation. The residues are linked by strong H^{α}–H^{N} sequential NOE contacts and have large coupling constants except for residues 80–83 where the polypeptide chain changes direction. The other loop has a more compact structure. The side chain of residue Leu-42 packs onto the ring of Trp-35. Although there is no regular secondary structure in this region, the amide protons of residues 45 and 46 both form hydrogen bonds to the carbonyl oxygen of residues 41 and 42, respectively, in all of the structures. This result is consistent with the observation that these protons are protected from exchange with solvent (Bycroft et al., 1990b). These residues form a small helix-like structure that is disrupted by a type II turn formed by residues 46–49.

The two loops pack against one another mainly via interactions between residues Tyr-78, Arg-83, Trp-35, Leu-42, and Ala-43.

The largest variations in the calculated structures are in the N-terminal region of the protein and in the major loops. When these regions are excluded, the average RMS deviation from the mean structure for residues 5–34, 50–56, 71–76, and 85–109 is 0.62 Å for the backbone atoms and 1.0 Å for all atoms. Loop regions are in general the least well-defined areas in NMR-derived structures (Clore & Gronenborn, 1989). Within these regions there is often a lack of short (<5 Å) interproton contacts to atoms in the rest of the molecule that could provide potential NOE interactions, and this can make it difficult to define the position of loops with respect to the main body of the protein (Clore et al., 1987). In addition, loop regions in proteins are often mobile, and this can result in a loss of NOE intensity as a result of motional averaging. In barnase, there are less NOEs in the loop regions compared to the rest of the protein (Figure 6). The least well-defined region in the protein is the loop between strands β-I and β-II

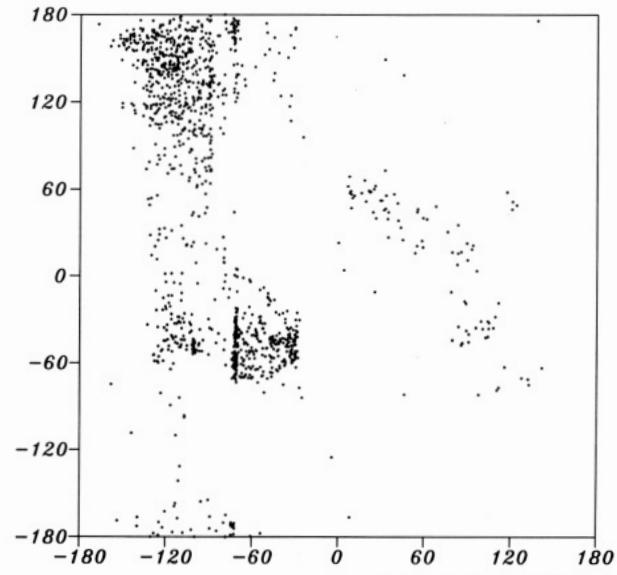

FIGURE 7: Ramachandran ϕ,ψ plot for residues 5–34, 50–56, 71–76, and 85–109 in the 20 solution structures of barnase.

of the β-sheet. The only NOE contacts with the rest of the protein are from protons in the side chain of Leu-63. In the rest of the loop, there are only interloop contacts between residues 58 and 61 and 63 and 56, and sequential NOE contacts.

The Ramachandran plot (Ramachandran & Sasisekharan, 1968) for the ϕ and ψ angles of residues 5–18, 50–56, 71–76, 85–100, and 105–109 is shown in Figure 7. The backbone angles in the structures lie within the limits normally found in proteins with the exception of residues 18, 58, 77, 94, 102, and 103, which have positive ϕ angles. Positive ϕ angles are relatively uncommon in proteins (Shultz & Schirmer, 1978). When positive ϕ angles are observed, they are most often seen for Gly and Asn residues. Two of the amino acids in barnase that have positive ϕ angles are Asn residues (58 and 77). Both of these residues are located in loops. His-102 and Tyr-103 are in a type III′ turn. The backbone of conformations of residues 18 and 94 are more unexpected. His-18 is at the end of an α-helix, and Trp-94 is at the end of a type I turn. We are currently investigating the effects of specific amino acid substitutions on the ϕ angles of these residues in an attempt to determine the factors that produce these backbone conformations.

Comparison to the Crystal Structure. The crystal structure of barnase has been solved (Mauguen et al., 1982), and so a comparison can be made between the structures produced by X-ray crystallography and by NMR. A superposition of the backbone atoms of the mean solution structure and the crystal structure is shown in Figure 8. A simple comparison of structures shows that the secondary structure and overall fold are similar. The average deviation between the structures is 1.8 Å for the main-chain atoms and 3.0 Å for all atoms. A comparison of the backbone torsion angles in the two structures shows that only five of the residues (Trp-35, Gly-61, Gly-65, Lys-66, and Gly-68) have ϕ angles that deviate more than 60° between the structures. These residues are all located within the loop regions of the protein. All of the residues that have positive ϕ angles in the NMR structure (His-18, Asn-58, Asn-77, Trp-94, His-102, and Tyr-103) have positive ϕ angles in the X-ray structure.

The agreement between the structures is best in the regions that contain regular secondary structure and worse in the loops. When the poorly defined regions of the NMR structure are

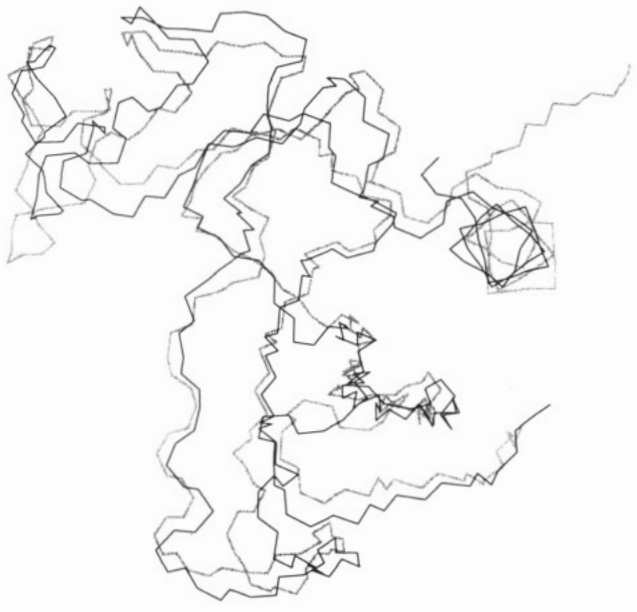

FIGURE 8: Superposition of the C^{α} atoms of the mean NMR structure of barnase and the X-ray structure. The NMR structure is in bold.

excluded from the comparison, the average deviation between the structures for residues 5–34, 50–56, 71–76, and 85–109 is 1.40 Å for the backbone atoms and 1.9 Å for all atoms. The regions where the largest deviations occur are also the least well-defined in the NMR structure. It is probable that these differences are a result of the lack of definition of the NMR structure in these areas rather than any significant variation between the two structures.

In conclusion, in the solution structure of barnase, the central core of the protein is well-defined, and, in this region, there is a close agreement between the NMR structures and the crystal structure. The conformation of the protein is, however, less well-defined in the relatively high proportion of barnase not involved in regular secondary structure.

ACKNOWLEDGMENTS

M.B. was the recipient of a European Molecular Biology Organisation short term fellowship. We gratefully thank Professor Guy Dodson and Dr. Chris Hill for the coordinates of the crystal structure of barnase.

REFERENCES

Arseniev, A., Schultze, P., Wörgötter, E., Braun, W., Wagner, G., Vasák, M., Kägi, J. H. R., & Wüthrich, K. (1988) *J. Mol. Biol. 201*, 637–657.

Brooks, B. R., Bruccoleri, R. E., Olafson, B. D., States, D. J., Swaminathan, S., & Karplus, M. (1983) *J. Comput. Chem. 4*, 187–217.

Brünger, A. T. (1988) XPLOR *Manual*, Yale University, New Haven, CT.

Bycroft, M., Matouschek, A., Kellis, J. T. Jr., Serrano, L., & Fersht, A. R. (1990a) *Nature (London) 346*, 488–490.

Bycroft, M., Sheppard, R. N., Lau, F. T. K., & Fersht, A. R. (1990b) *Biochemistry 29*, 7425–7432.

Chothia, C., (1984) *Annu. Rev. Biochem. 53*, 537–572.

Clore, G. M., & Gronenborn, A. M. (1989) *CRC Crit. Rev. Biochem. Mol. Biol. 24*, 479–564.

Clore, G. M., Gronenborn, A. M., Kjaer, M., & Poulsen, F. M. (1987) *Protein Eng. 1*, 305–311.

Ernst, R. R., Bodenhausen, G., & Wokaun, A. (1987) *Principles of Nuclear Magnetic Resonance in One and Two Dimensions*, Clarendon Press, New York.

Hartley, R. W. (1989) *Trends Biochem. Sci. 14*, 450–454.

Havel, T. F. (1986) DISGEO, Quantum Chemistry Program Exchange No. 507, Indiana University, Bloomington, IN.

Hill, C., Dodson, G., Heinemann, U., Saenger, W., Mitsui, Y., Nakamura, K., Borisov, Tischenko, G., Polyakov, K., & Pavlovsky, S. (1983) *Trends Biochem. Sci. 8*, 364–369.

Jeener, J., Meier, B. H., Bachmann, P., & Ernst, R. R. (1979) *J. Chem. Phys. 71*, 4546–4553.

Jones, T. A. (1978) *J. Appl. Crystallogr. 11*, 268–272.

Karplus, M. (1963) *J. Am. Chem. Soc. 85*, 2870–2871.

Kellis, J. T., Jr., Nyberg, K., Sali, D., & Fersht, A. R. (1988) *Nature (London) 333*, 784–786.

Kellis, J. T., Jr., Nyberg, K., & Fersht, A. R. (1989) *Biochemistry 28*, 4914–4922.

Kline, A. D., Braun, W., & Wüthrich, K. (1988) *J. Mol. Biol. 204*, 675–724.

Ludvigsen, S., Andersen, K. V., & Poulsen, F. M. (1991) *J. Mol. Biol. 217*, 731–736.

Marion, D., & Wüthrich, K. (1983) *Biochem. Biophys. Res. Commun. 113*, 967–974.

Matouschek, A., Kellis, J. T., Jr., Serrano, L., & Fersht, A. R. (1989) *Nature (London) 340*, 122–126.

Matouschek, A., Kellis, J. T., Jr., Serrano, L., Bycroft, M., & Fersht, A. R. (1990) *Nature (London) 346*, 440–445.

Mauguen, Y., Hartley, R. W., Dodson, E. J., Dodson, G. G., Bricogne, G., Chothia, C., & Jack, A. (1982) *Nature (London) 297*, 162–164.

Mossakowska, D., Nyberg, K., & Fersht, A. R. (1989) *Biochemistry 28*, 3843–3850.

Nilges, M., Gronenborn, A. M., & Clore, G. M. (1988) *FEBS Lett. 229*, 317–324.

Paddon, C. J., & Hartley, R. W. (1987) *Gene 53*, 11–19.

Pardi, A., Biliter, M., & Wüthrich, K., (1984) *J. Mol. Biol. 180*, 741–751.

Piantini, U., Sørensen, O. W., & Ernst, R. R. (1982) *J. Am. Chem. Soc. 104*, 6800–6803.

Ramachandran, G. M., & Sasisekharan, V. (1968) *Adv. Protein Chem. 23*, 283–437.

Rance, M., Sørensen, O. W., Bodenhausen, G., Wagner, G., Ernst, R. R., & Wüthrich, K. (1983) *Biochem. Biophys. Res. Commun. 117*, 479–485.

Richardson, J. (1981) *Adv. Protein Chem. 34*, 167–339.

Sali, D., Bycroft, M., & Fersht, A. R. (1988) *Nature (London) 335*, 740–743.

Schultz, G. E., & Schirmer, R. H. (1978) *Principles of Protein Structure*, Springer-Verlag, Berlin.

Serrano, L., & Fersht, A. R. (1989) *Nature (London) 342*, 296–298.

Sevcik, J., Sanishvili, R. G., Pavlovsky, A. G., & Polyakov, K. M. (1990) *Trends Biochem. Sci. 15*, 159–162.

States, D. J., Haberkorn, R. A., & Ruben, D. J. (1982) *J. Magn. Reson. 48*, 286–292.

Venkatachalam, C. M. (1968) *Biopolymers 6*, 1425–1436.

Wagner, G., Braun, W., Havel, T. F., & Wüthrich, K. (1987) *J. Mol. Biol. 182*, 295–315.

Wüthrich, K. (1986) *NMR of Proteins and Nucleic Acids*, Wiley, New York.

Wüthrich, K. (1989) *Science 243*, 45–50.

Zuiderweg, E. R. P., Boelens, R., & Kaptein, R. (1985) *Biopolymers 24*, 601–611.